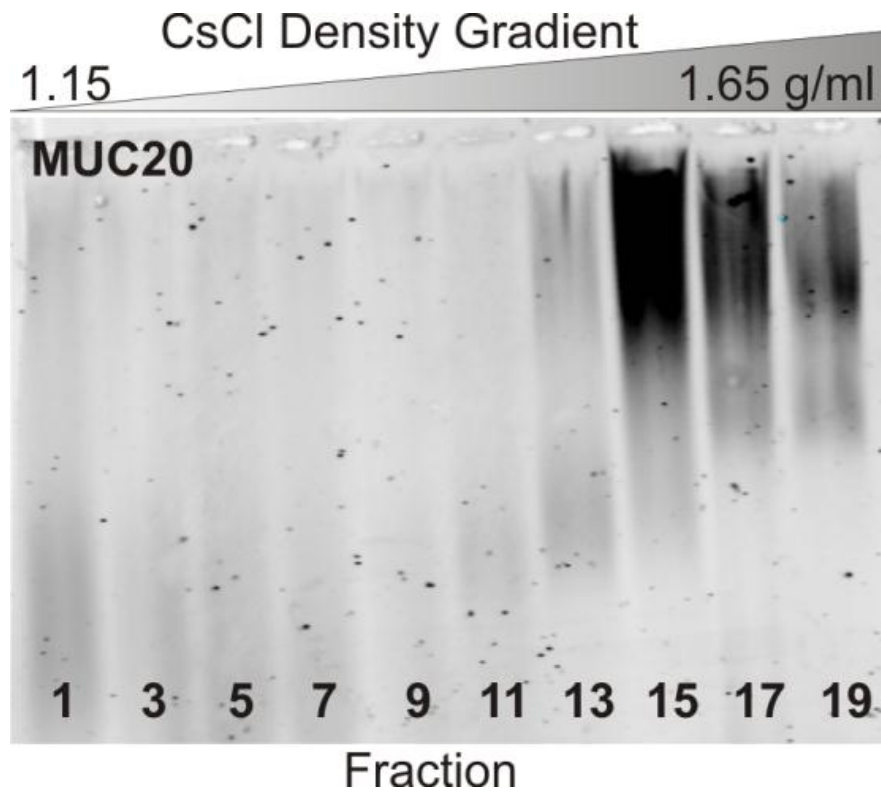
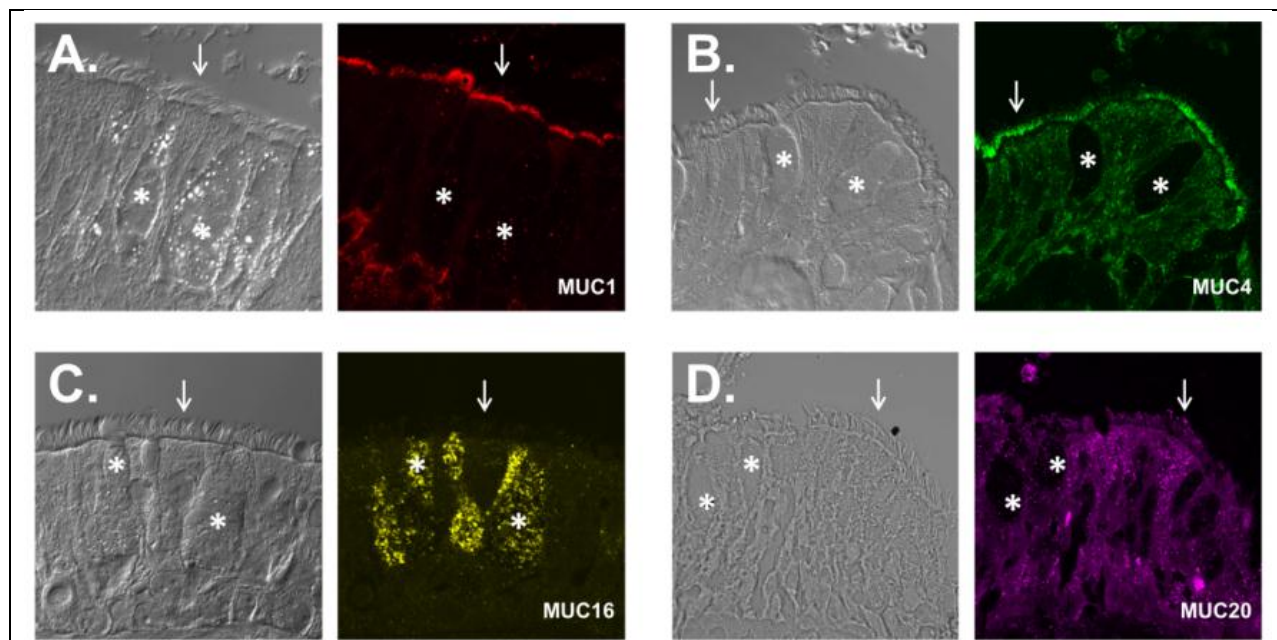


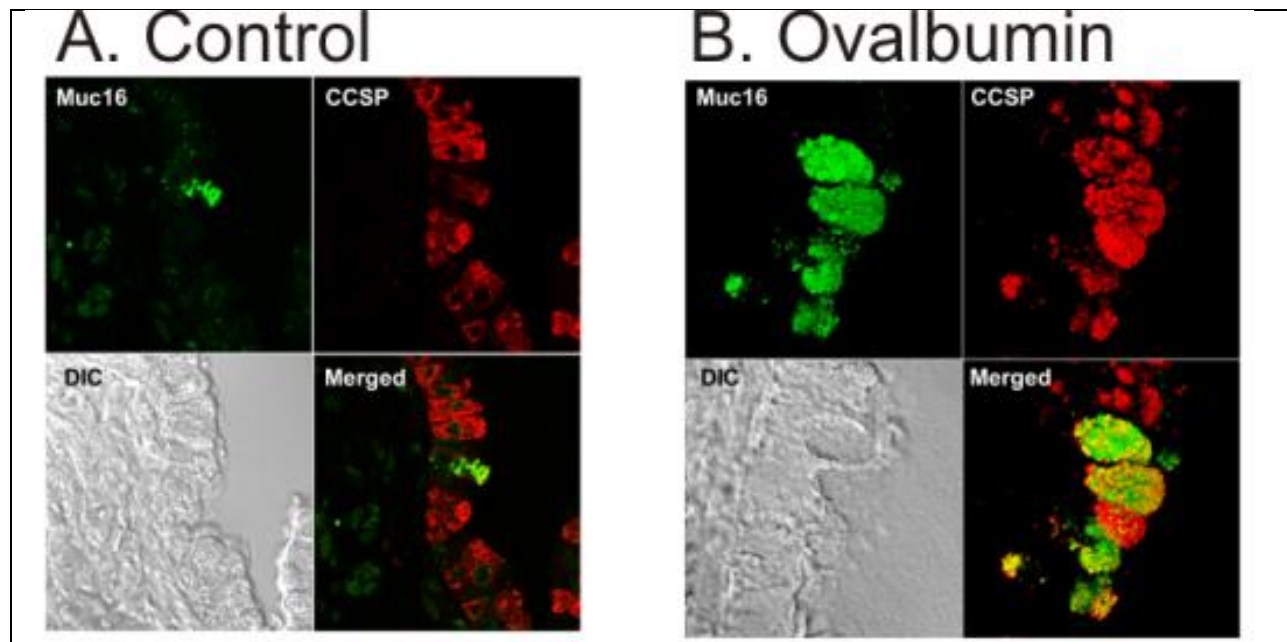
Supplemental Figure S1. KS and tethered mucins expressed in airway epithelia. Panels A-C. KS, MUC4, and MUC1 expression in superficial epithelia. Panel A, human bronchus probed with a KS antibody. Panel B, HTBE cell culture probed with a MUC4 antibody targeting the VNTR domain, which detects the mucin selectively in the ER. Panel C, human bronchus probed with antibodies targeting extracellular epitopes in non-glycosylated domains of MUC1 (red) and MUC4 (green). **Panels D-F, MUC1, MUC16, and MUC20 expression in submucosal glands of human bronchus.** Panel D, a cross-section through gland acini probed for MUC1; DIC + fluorescence, DAPI counterstain. Panel E, longitudinal section (left, fluorescence only) and cross-section (right, DIC + fluorescence) through mucous acini probed for MUC5B and/or MUC16, as indicated, using antibodies as in Figure 5. Panel F, a cross-section through mucous acini probed for MUC20, DIC + fluorescence, DAPI counterstain. Scale bars = 10 μm.



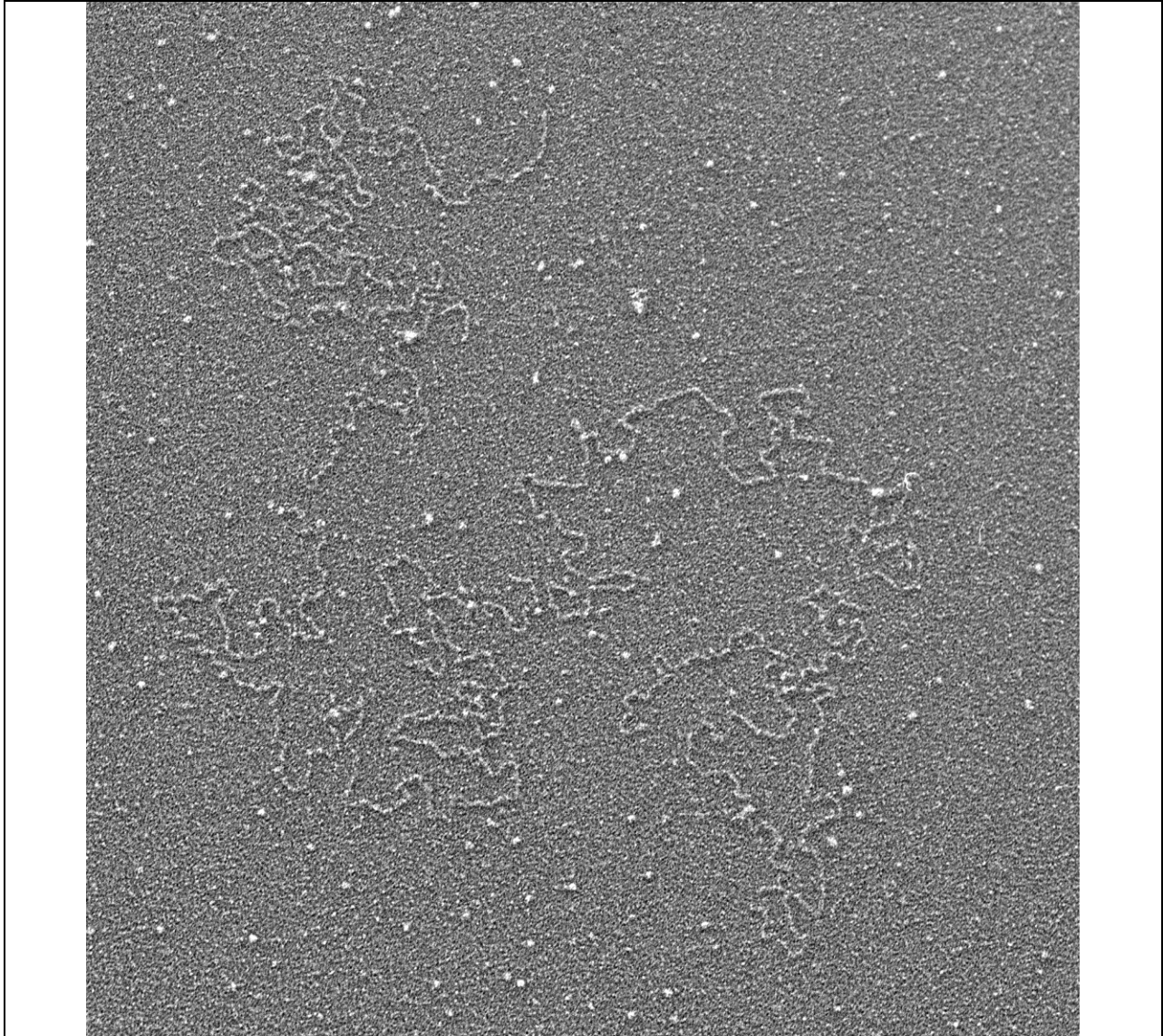
Supplemental Figure S2. Agarose Western Blot showing CsCl gradient fractions probed for antibody to MUC20. HTBE cell culture secretions were solubilized in GuHCl and separated on a CsCl density gradient similar to the one shown in Figure 3. Subsamples of alternate fractions were further separated by electrophoresis on 1% agarose, transferred by vacuum blotting to nitrocellulose, and probed with a polyclonal antibody to MUC20.



Supplemental Figure S3. Tethered mucins of human bronchial epithelium – II. A. *MUC1*; B. *MUC4*; C, *MUC16*; D, *MUC20*. Each mucin is shown in a matched pair of DIC(Nomarski) and fluorescent images. Arrows indicate example ciliated cells, asterisks mark example goblet cells. In Panel C, note the granular pattern of staining, indicating co-localization of MUC16 in mucin granules. Cilia, $\sim 7 \mu\text{m}$, serve to indicate scale.

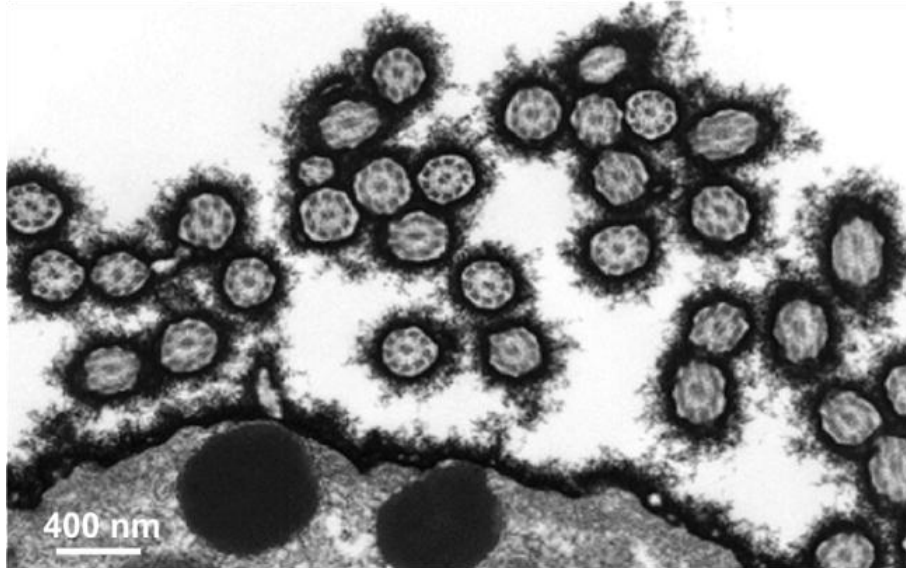


Supplemental Figure S4. Muc16 expression in murine airways of, (A) control wildtype mice and (B) mice with allergic, mucous metaplasia induced by treatment with ovalbumin. Sections were co-stained with antibodies to MUC20 and CCSP. Note the abundance of CCSP-stained, Clara cells in the control airways, relative to Muc16-stained cells, a result consistent with a low level of Muc5b expression (see Zhu, et al., 2008. *J Physiol.* 586:1977-1992). In contrast, Muc16 is upregulated and clearly co-expressed with CCSP in Clara/goblet cells in the ovalbumin-exposed mice, again consistent with the upregulation of polymeric mucins in mucus metaplasia. Note the obvious granular staining pattern of Muc16 staining in panel B, suggesting co-localization in mucin granules.



Supplemental Figure S5. Electron micrograph of the linearized form of MUC5B. Sample prepared as for Figure 4. For more images and details on the linearization/maturation of polymeric mucins, see Kesimer, et al., 2010, *Am J Physiol* 298:L15-22 (Reference # 18).

A. Mouse Cilia, Ruthenium Red



Supplemental Figure S6. Mucosal glycocalyx of mouse airways visualized by conventional EM and ruthenium red staining. The image shows cilia in cross-section, projected over the surface of a Clara cell.